

Infrared Spectrum of the Nitrosyl Chloride Monomer and Dimer in Solid Nitrogen: Temperature-Induced Mobility of Nitrosyl Chloride

L. Schriver-Mazzuoli,^{*,†} A. Hallou, and A. Schriver

Laboratoire de Physique Moléculaire et Applications,[‡] Unité propre du CNRS Université Pierre et Marie Curie, Tour 13, case 76, 4 place Jussieu, 75252 Paris Cedex 05, France

Received: July 13, 1998; In Final Form: September 14, 1998

Experimental investigations at different temperatures of the infrared spectra of nitrosyl chloride trapped in a nitrogen matrix allow identification of the ClNO dimer and a next nearest neighbor pair. At 21 K, the pair transforms irreversibly in monomer and also in dimer according to the ClNO initial concentration, whereas at 26 K, the monomer transforms to dimer. On the basis of kinetic studies, these observations have been interpreted by the existence of two distinct motions of the ClNO molecule in the nitrogen matrix: the first at short range with an activation energy of around 4 kJ mol⁻¹, and the second at long range leading to the formation of (ClNO)₂ with an activation energy of around 7.5 kJ mol⁻¹.

Introduction

A knowledge of thermal mobility and diffusion of species in matrixes is important in order to understand how these dynamical processes affect the rates of a variety of reactions in this medium. Several years ago the mobility of small atoms such as N, O, F, and S were qualitatively established,^{1–5} and more recently it has been quantitatively characterized in particular for the oxygen atom.^{6–13} Diffusion-limited geminate recombination of O + O₂ in solid xenon was observed between 14 and 25 K, and an activation energy for diffusion of O atoms was calculated of 2.0 ± 0.5 kJ mol⁻¹.¹² In crystalline Kr and Xe, Danilychev and Apkarian showed that atomic oxygen mobility was characterized by long-range migration with migration lengths of ≥300 Å.¹⁰ By monitoring the 736 nm emission from XeO excimers, Krueger and Weitz¹¹ gave evidence for a bimodal distribution of diffusion coefficients; a first mode corresponded to a fast rate due to defects and inhomogeneity in the matrix, and a second mode was associated with a lower migration rate. Recently in this laboratory, it has been shown that in a nitrogen matrix two distinct oxygen atom diffusion processes occur: a first one at short distance between 14 and 20 K and a second one at longer distance which requires a higher temperature.¹³ Thermal diffusion in matrixes of small molecules has also been investigated. F. Legay and N. Legay have calculated the diffusion coefficient of NO in nitrogen and neon matrixes from the rate of dimer formation.^{14,15} More recently, mobility of HBr in solid xenon was studied by monitoring the formation of dimers as a function of both the initial deposition temperature and subsequent annealing treatment.¹⁶ As suggested by theory¹⁷ and previous experimental investigations^{13,18} the HBr diffusion at long range depends on matrix morphology and consequently on deposition temperature, the lower deposition temperature favoring defects and inhomogeneity in the matrix.

In this work, extensive temperature studies on the vibrational spectrum of ClNO trapped in nitrogen matrixes are reported.

An additional band in the monomer spectral regions which was assigned to a next nearest neighbor dimer has offered a rare opportunity to study experimentally in detail the diffusion of the nitrosyl chloride. Variations in intensity of monomer and dimer bands with temperature have allowed us to confirm the existence of two distinct motions of species in nitrogen matrixes, as we suggested previously.¹³

Nitrosyl chloride has attracted considerable interest because of its unusual structure (long halogen–nitrogen and short nitrogen–oxygen bond lengths) leading to a positive charge on the N atom.¹⁹ Infrared spectra of nitrosyl chloride isolated in rare gas solids have been studied in detail by Jones and Swanson.²⁰ Later, as a part of our studies of the ClNO:HCl complex²¹ and of the photodissociation of ClNO,²² the vibrational spectrum of natural and isotopic ClNO in nitrogen and argon has been described.

Experimental Section

A closed-cycle helium refrigerator (Air Product Displex model 202 A) was used. The Microprocessor-based digital Temperature Indicator/Controller (Scientific Instrument 9600-1) measures and displays process temperature via a remote calibrated silicon diode temperature sensor and controls power to a heater within the refrigeration system to maintain process temperature at a predetermined setpoint value: the resolution is 0.1 K. In the chosen temperature range (11 to 30 K) the accuracy of the measurements is ±0.5 K, the controllability is ±0.2 K, and the repeatability is ±0.2 K.

ClNO (Merck Suchardt) was condensed at 77 K and subjected to several freeze thaw cycles prior to sample preparation. ClNO is approximately 1% dissociated at room temperature, and we do not remove impurities such as NO and NO₂. Gas mixtures were prepared by standard manometric techniques and sprayed onto a gold-plated copper mirror. The ClNO/N₂ ratio was in the range 1/1000 to 1/10 000. The deposition temperature was 17 K, and the deposition rate was generally of 10 mmol/h.

Spectra were recorded at 11 K or higher temperatures with a 0.5 cm⁻¹ resolution over the 4000–300 cm⁻¹ range in a reflection mode (double transmission) using a Fourier transform infrared spectrometer (Bruker IFS 113 v).

* Author to whom correspondence should be addressed.

† Also at Université Paris XIII (Laboratoire d'Etude des Nuisances Atmosphériques).

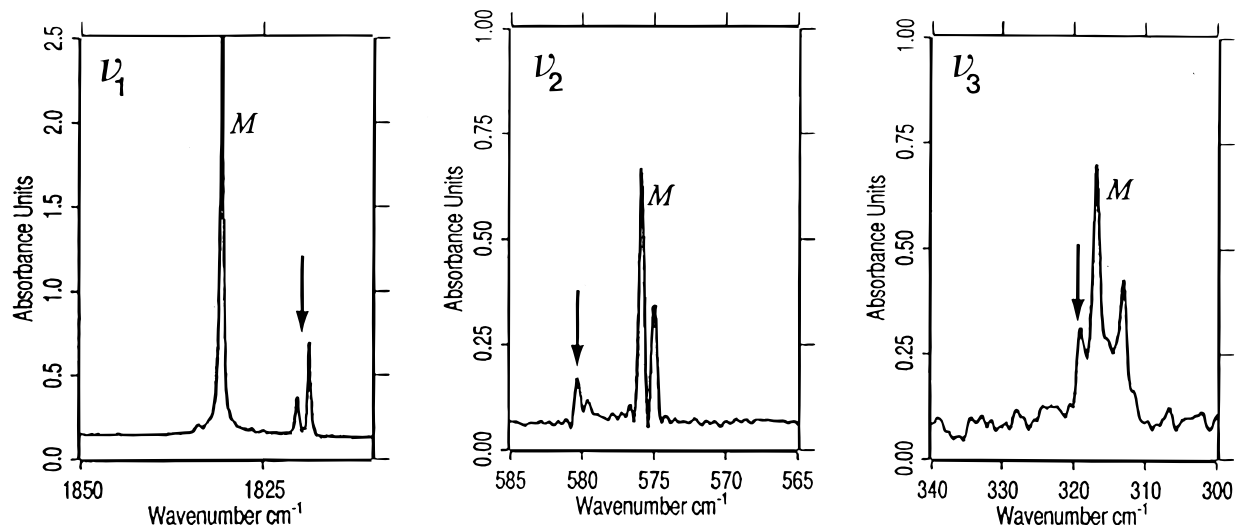


Figure 1. FTIR spectrum recorded at 11 K in the ν_1 , ν_2 , and ν_3 fundamental spectral nitrosyl chloride regions of a ClNO/N₂ (1/10 000) sample. Additional bands appearing near the monomer absorptions (M) are indicated by arrows.

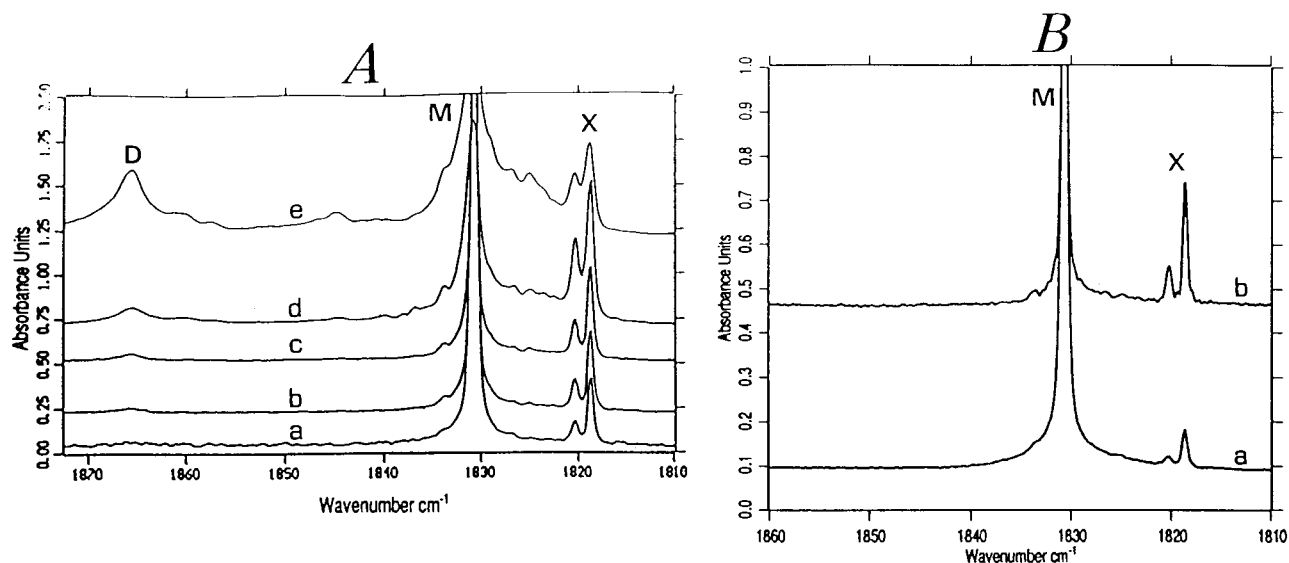


Figure 2. (A) ClNO concentration effects on ν_{NO} IR spectra in nitrogen matrixes. Spectra were recorded at 11 K just after deposition at 17 K. (a) ClNO/N₂ 1/10 000, (b) ClNO/N₂ 1/5000, (c) ClNO/N₂ 1/3000, (d) ClNO/N₂ 1/1000, (e) ClNO/N₂ 1/500. For comparison, the harmonic $2\nu_1$ of M was adjusted at the same intensity. (B) FTIR spectra in the ν_{NO} region obtained for 1/10 000 ClNO/N₂ mixtures initially deposited at (a) 11 K, (b) 17 K. Spectra were recorded at 11 K.

Results

1. Vibrational Spectrum of the ClNO Molecule. Temperature and Irradiation Effects. The nitrosyl chloride is a near-prolate asymmetric molecule whose fundamentals ν_1 , ν_2 , and ν_3 are measured in a nitrogen matrix at 1830.7 cm⁻¹, 575.8 cm⁻¹ (³⁵Cl)–575.0 cm⁻¹ (³⁷Cl), and 316.7 cm⁻¹ (³⁵Cl)–313.0 cm⁻¹ (³⁷Cl), respectively. Due to substantial mixing between the bending mode and the N–Cl stretching, assignment of the ν_2 and ν_3 to one of these modes is not straightforward and differs from one report to another. In this work we have chosen the classification previously adopted;²¹ i.e., ν_2 should be labeled the N–Cl stretching mode and ν_3 labeled the bending mode. In the course of our investigations of nitrosyl chloride water complex in nitrogen matrixes²³ our attention was attracted by the appearance of additional weak bands in all fundamental harmonic and combination regions of the ClNO molecule, even at high dilution. Their frequencies are reported in Table 1, column 2, and compared to the corresponding monomer frequencies. As shown in Figure 1, in the ν_{NO} region, the additional component was red-shifted by 12 cm⁻¹ from the

TABLE 1: Absorptions (cm⁻¹) Observed in Nitrogen Matrix for the ClNO Monomer (M) and for the X and D Species

mode	M	X	D
ν_1	1830.7	1820.4–1818.7	1865.5
ν_2	575.8–575.0	580.3–579.6	568.2
ν_3	316.7–313.0	319.2	312.5
$2\nu_1$	3626.0	3601.7	3679.2
$\nu_1 + \nu_2$	2407.3–2406.3	2399.7	2417.9
$\nu_1 + \nu_3$	2147.4–2143.3	2137.7–2133.8	2167.1–2164.0
$\nu_2 + \nu_3$	889.4–884.6	896.2	

monomer band, while in the $\nu_{\text{N-Cl}}$ and δ_{NOCl} fundamental regions they were blue-shifted by 4.5 and 2.5 cm⁻¹, respectively, from the corresponding monomer bands. The species responsible for these features (hereafter labeled X) which contains one ClNO molecule at least is not due to a complex between ClNO and impurities such as Cl₂, NO, and NO₂ as revealed by subsequent double doping experiments with ClNO and Cl₂, NO, and NO₂ in nitrogen.

As illustrated in Figures 2 and 3 in the ν_{NO} region, the behavior of the X band depended on the initial M/R values,

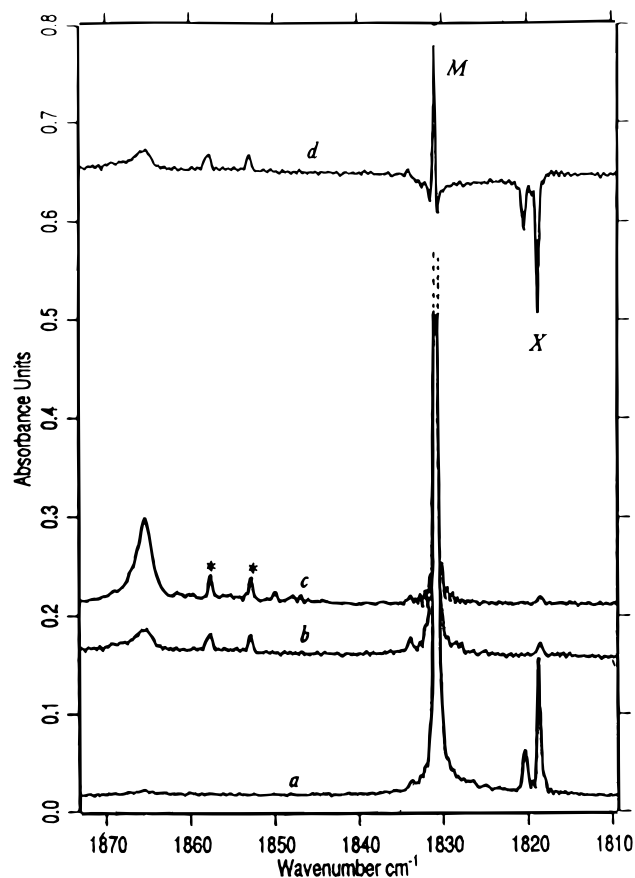


Figure 3. FTIR spectra in the ν_{NO} region of a 1/10 000 CINO/ N_2 matrix initially deposited at 17 K (a) and annealed at 23 K during 30 min (b) and at 27 K during 5 min (c). All spectra were recorded after cooling the matrix at 11 K. Trace (d) is the difference spectrum of (b) and (a) spectra. * indicates impurity bands due to CINO complexed by H_2O traces.

on the deposition temperature, and on annealing temperature.

Figure 2A shows spectra recorded at 10 K after deposition at 17 K for various M/R ratios. For comparison the harmonic $2\nu_1$ of the monomer labeled M measured at 3626 cm^{-1} was adjusted to the same intensity for the different samples. It can be seen that the intensity of the X doublet increases for M/R from 10 000 to 1000, then decreases for M/R 500. In parallel a relatively broad band (full width at half-maximum $\text{fwhm} = 2.3\text{ cm}^{-1}$) located to 1865.4 cm^{-1} (labeled D) which existed as traces for M/R 10 000 grows strongly with concentration. Absorptions responsible for the D species were observed in all regions of the CINO molecules, which indicates that D contains at least, as the X species, one CINO molecule. Their frequencies are summarized in Table 1, column 3.

Figure 2B shows the effect of initial deposition temperature (11 and 17 K) for a matrix sample of M/R = 10 000. In the spectrum recorded after deposition at 11 K, the relative intensity of the monomer band in regard to the intensity of the X band is stronger than that measured in the spectrum recorded after deposition at 17 K.

Figure 3 displays spectra of a dilute sample (CINO/ $\text{N}_2 = 1/10\ 000$) recorded at 11 K: (i) after deposition at 17 K (trace a); (ii) after warming the matrix to 23 K for twenty minutes (trace b); (iii), after annealing at 28 K (trace c). The X band disappears irreversibly at 23 K, while the D band grows strongly after annealing at 28 K. The difference spectrum of the matrix sample recorded at 11 K after annealing to 23 K and the matrix

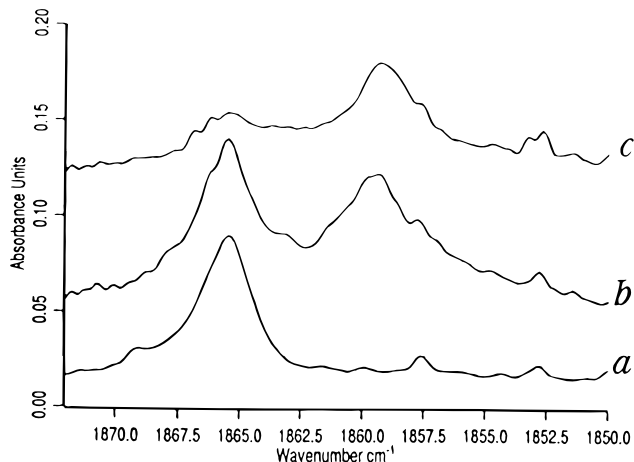


Figure 4. Comparison in the $1870\text{--}1850\text{ cm}^{-1}$ spectral region between the spectrum of natural CINO species (CINO/ N_2 1/1000) (a) and two mixed samples containing $\text{Cl}^{14}\text{N}^{16}\text{O}$ and $\text{Cl}^{15}\text{N}^{16}\text{O}$ at different ratios, (b) mixture $\text{Cl}^{14}\text{N}^{16}\text{O}/\text{Cl}^{15}\text{N}^{16}\text{O}$ 1/0.4, and (c) mixture $\text{Cl}^{14}\text{N}^{16}\text{O}/\text{Cl}^{15}\text{N}^{16}\text{O}$ 0.7/1.

sample recorded at 11 K after deposition as presented in Figure 3 (trace d) shows that the disappearance of the X band is accompanied mainly by the growth of the D band with a weak increase in intensity of the M band. The difference spectrum of the matrix sample recorded after annealing to 23 K and the matrix sample recorded after annealing to 28 K (not represented) shows that the D band grows as the intensity of the monomer band decreases.

Other experiments showed that the X band began to disappear from 21 K, whereas the D band grew from monomer band only above 26 K. After the disappearance of the X band, no evolution of the spectrum was observed between 20 and 26 K.

Accurate measurements of ν_{NO} band absorbances of CINO monomer disappearing with temperature (above 26 K) and the D band absorbance appearing at the same time showed that the intensity ratio of D and M was 0.5 ($A_{1865.4}/A_{1830.7} = 0.5$). From this result, the ratio between the X intensity and M intensity in ν_{NO} region was calculated from the disappearance below 23 K of X into M and D. It was found to be 1.2 ± 0.2 .

Spectra of two mixed samples (CINO/ N_2 1/1000) containing natural and ^{15}N -enriched CINO at different ratios (1/0.4 for the first sample and 0.7/1 for the second sample) were also recorded. After deposition, in the ν_{NO} region of $\text{Cl}^{14}\text{N}^{16}\text{O}$, the X band was observed at the same position, whereas a new band at 1859.3 cm^{-1} appeared near the D band located at 1865.4 cm^{-1} . As shown in Figure 4 the relative intensity of the 1859.3 cm^{-1} absorption with respect to the other one increased with $\text{Cl}^{15}\text{N}^{16}\text{O}$ abundance. In the $\nu(^{15}\text{N}^{16}\text{O})$ region (not represented), the X band at $1789.1\text{--}1787.5\text{ cm}^{-1}$ did not show any splitting and the two corresponding bands of D were overlapped by the ν_{NO} of CINO monomer which was now characterized by two shoulders at both sides situated at about 1833 and 1827 cm^{-1} respectively.

To see if a conversion of X into D or D into X could occur by irradiation, a matrix containing CINO 1/10 000 was irradiated in different wavelength ranges (IR and V-UV), first after deposition (presence of only the X band) then after annealing to 28 K (presence of only the D band). No conversion was observed but as illustrated Figure 5 in the ν_{NO} region a different behavior was observed for the X_{NO} and D_{NO} bands. The X absorption was insensitive to irradiation in all irradiation domains, whereas the D band vanished under UV irradiation with a mercury medium-pressure lamp and with the 266 nm

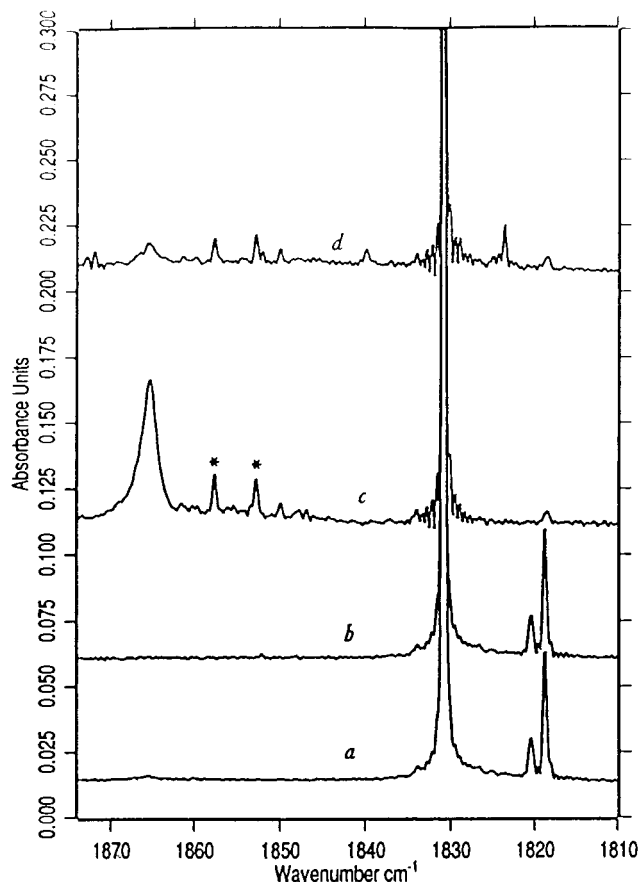


Figure 5. Comparison of the spectra in the ν_{NO} region before irradiation (a) and (c) and after irradiation at 11 K with the 266 nm laser line during 60 min (b) and (d). (a) CINO/N₂ 1/10 000 sample, (b) irradiation of (a) sample, (c) CINO/N₂ 1/2000 sample annealed to 28 K then recooled to 11 K, (d) irradiation of (c) sample. * indicates bands due to CINO:H₂O complex.

laser line with the appearance of two new features at 1839.9 and 1823.6 cm^{-1} (not identified) and the increase of NO monomer which existed as traces after deposition.

2. Quantitative Temperature Studies. To analyze accurately the temperature effect on the D, M, and X bands, two sets of experiments were performed. The first one was designed to probe the time dependence of the X band for a matrix deposited and held to 21 K, then to 22 and to 23 K. In the second one, the sample was annealed to 23 K until the X band disappeared. Then the matrix was held to 26, 27, and 28 K in order to pay attention to the evolution of the D band over time.

Evolution of the X Band. Kinetic studies of the disappearance of X at 21, 22, and 23 K were carried out on matrixes containing relatively high concentrations of CINO (CINO/N₂ = 1/1000). This concentration was needed for obtaining at the initial time a substantial intensity of the X band. At this concentration as shown in Figure 6A where typical spectra in the ν_{NO} region are recorded at 23 K, the D band was also present at the initial time ($t = 0$). Furthermore at the studied temperatures the X band is broader than at 11 K, and its frequency is blue-shifted involving a weak overlapping with the monomer band. Consequently measurements of the intensity of X and D bands at each time t were made in the ν_{NO} region on the difference spectrum of the spectrum recorded at $t = \infty$ and of the spectrum at time t for the X band and of the spectrum recorded at $t = 0$ and of the spectrum recorded at time t for the D band. The ν_{NO} band at 1830.0 cm^{-1} of the monomer was not chosen for monitoring its evolution because its optical density was more

than 0.8. Consequently intensity measurements of the M band were made directly from the main component of the $\nu_1 + \nu_3$ combination which was located at 2147.1 cm^{-1} for the studied temperature. The ratio between the ν_{NO} monomer band absorbance and the $\nu_1 + \nu_3$ monomer combination band absorbance was found to be 90 ± 5 . Figure 6B shows the evolution at 23 K of the three species in the ν_{NO} region with time. If we take into account the intensity ratios of the different bands, it can be seen that the disappearance of X is well correlated to the growth of M plus D. Note that the present yield of D, in regard to M, depends on the initial concentration of CINO. In a very highly dilute sample, only growth of the monomer was observed.

The disappearance of X was found to be a first-order process for the three studied temperatures. Figure 7 shows plots of $\ln A_x^0/A_x$ versus time for the three temperatures, where A^0 is the intensity of the X band at $t = 0$. From the slope of the linear curves, rate constants were found to be $(2.2 \pm 0.1) \times 10^{-4} \text{ s}^{-1}$, $(9.8 \pm 0.2) \times 10^{-4} \text{ s}^{-1}$, and $(23 \pm 1) \times 10^{-4} \text{ s}^{-1}$ for 21, 22, and 23 K, respectively.

Evolution of the D Band. As mentioned previously, after the disappearance of the X band, no evolution of the monomer and D absorptions was observed until 26 K. Consequently, kinetic studies were carried out at 26, 27, and 28 K. The concentration of CINO in nitrogen was chosen to be 1/2000. Figure 8 shows the evolution with time of monomer and dimer bands in the ν_{NO} region at 26 K. As can be seen, the decrease of CINO monomer is very weak and is well correlated with the increase of the D band if we taking into account that the ratio $I_{1830.7}/I_{1865.4}$ is equal to 2. After 21 h, only 25% of the monomer band had disappeared. At 27 and 28 K, similar curves were obtained but the formation of D from M increased with temperature: 30% of monomer disappeared after 7 h at 27 K and after 2 h at 28 K.

The decrease of the monomer was not a first-order process and will be discussed in the following section.

Discussion

1. Identification of the D and X Species. The characteristic bands of the D species which increase in intensity with CINO concentration and annealing can be assigned without ambiguity to the CINO dimer. In the ν_{NO} region the shift of the D band in regard to the monomer band (35 cm^{-1}) is similar to the shift observed by Jones et al. in argon²⁰ for this species (36.3 cm^{-1}). Existence of one band in all fundamental regions, as in argon, suggests that the dimer is centrosymmetric with two equivalent subunits, an interpretation which seems to be confirmed by isotopic experiments. The 1865.4 cm^{-1} absorption assigned as the antisymmetric NO stretch in the pure dimer was found at 1865.4 cm^{-1} , whereas decoupled vibrations gave rise to the band at 1859.3 cm^{-1} for Cl¹⁴N¹⁶O–Cl¹⁵N¹⁶O mixed dimers in the ν (¹⁴N¹⁶O) region. The observed red shift (6.1 cm^{-1}) could indicate that the frequency of the in-plane NO stretch in the pure dimer is lower than the out-of-plane corresponding mode and could be situated at about 1853 cm^{-1} .

Identification of X which shows neither dimer behavior nor monomer behavior according to the experimental conditions is not straightforward. The observed dependence of the intensity ratio of monomer and X band with the deposition temperature and the conversion of X into D under 26 K which does not occur from monomer excludes the assignment of X to a monomer trapped in a metastable site. At first sight the disappearance of X from 23 K and in parallel, the appearance of D suggests that X could be a metastable dimer. However,

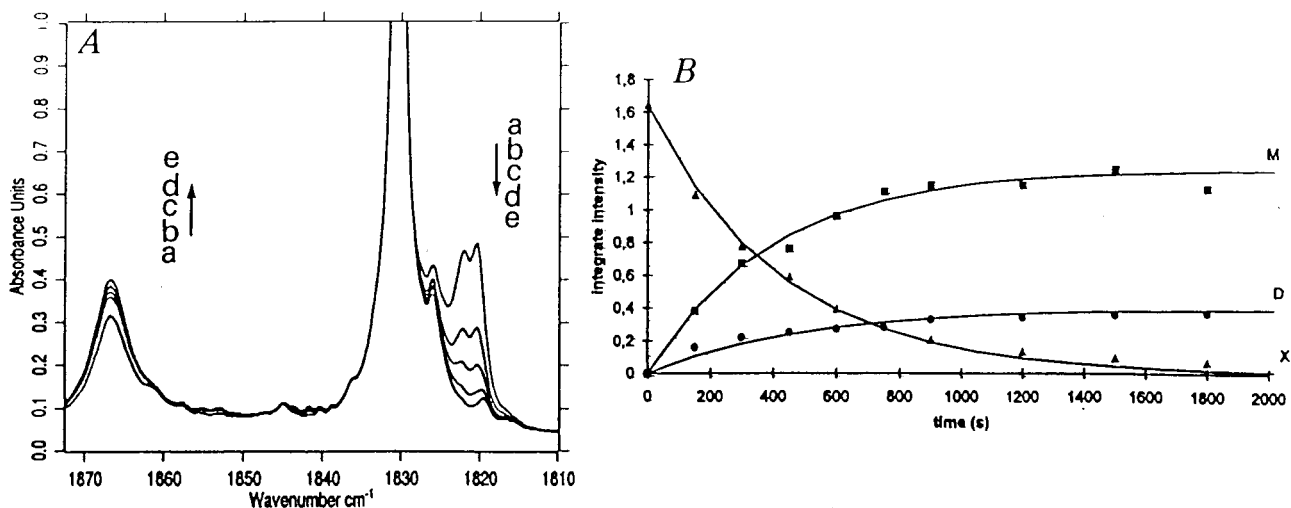


Figure 6. (A) Spectral changes with time at 23 K in the ν_{NO} region of a CINO/ N_2 1/1000 mixture (a) $t = 0$ min, (b) $t = 5$ min, (c) $t = 10$ min, (d) $t = 20$ min, (e) $t = 40$ min. (B) Time evolution at 23 K of ν_{NO} integrated intensity for monomer (M) and for D and X species (CINO/ $\text{N}_2 = 1/1000$).

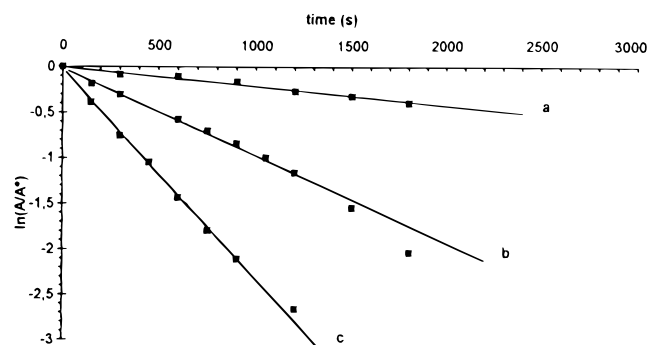


Figure 7. Plots of $\ln(A/A^0)$ versus sample storage time at 21 K (a), 22 K (b), 23 K (c); A^0 : ν_{NO} integrated intensity of X product at initial time; A: ν_{NO} integrated intensity of X product at time t (CINO/ $\text{N}_2 = 1/1000$).

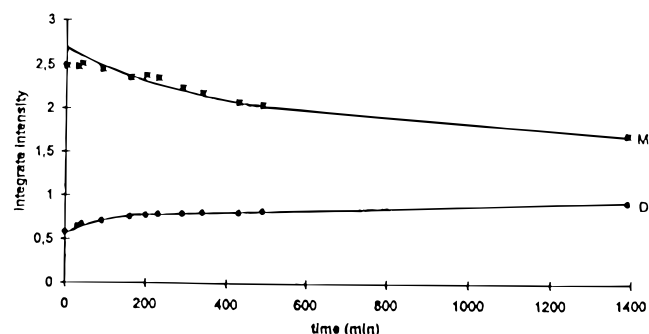


Figure 8. Time evolution at 26 K of ν_{NO} integrated intensity for monomer (M) and D product (CINO/ $\text{N}_2 = 1/2000$).

X transforms principally into M at low CINO concentration and this behavior does not appear compatible with this assumption. The contradictory properties of X are apparent only if one considers the possibility for a next nearest neighbor to be formed. This hypothesis accounts for all observed effects and in particular for the temperature behavior of X as discussed below. Frequency shifts of CINO in this pair (X) in regard to the monomer is of great interest. Indeed, in all complexes involving CINO (see ref 23 and references therein) as in the dimer, a blue shift of ν_{NO} and a red shift of ν_{NCl} are observed. Reverse shifts characterizing the CINO in the pair and the nonisotopic effect are an indication that the orientation of the two CINO molecules in nearest neighbor positions is very

different from that of the dimer. The structure of the dimer from other isotopic studies and the structure of the pair will be discussed in a forthcoming paper.

2. Diffusion of the CINO Molecule. Disappearance of the nearest neighbor dimer (X) from 21 K and the formation of a CINO molecule above 26 K appear as a direct consequence of the mobility of CINO in the matrix. The evolution of the X and monomer species with temperature suggests, as previously reported,¹³ two different mobility processes: a short-range diffusion occurring between 21 and 23 K leading to dissociation of the pair, and another process at longer range occurring from 26 K and leading to the formation of dimers from monomers. However, if the second process corresponds without ambiguity to a real diffusion of CINO monomer, the assumption of a short-range mobility of CINO at 21 K from our experimental results as discussed below is only tentative. Confirmation from molecular dynamics calculations would be useful.

Mobility of CINO at 21 K. Due to its size, the CINO molecule is assumed to be in a doubly substitutional site inducing a lattice distortion. A temperature increase to 21 K causes a rearrangement of the distorted matrix and the restabilization energy which is concentrated in the close vicinity of the trapped molecule could lead to the possibility for the monomer to move from its initial site to another nearby site. In the pair (X) two monomer molecules are close together. A jump for each monomer of the pair from one site to another causes the disappearance of the pair and an increase in isolated monomer. When the nitrosyl chloride concentration increases, the probability that one monomer molecule encounters another monomer molecule in its vicinity is increased and formation of dimer (D) is also observed. In this view two questions arise: (i) why do the two monomer molecules in the pair not move toward each other to produce the dimer? and (ii) how does the displacement of a CINO molecule from its double site to a nearest double site occupied by two nitrogen molecules occur? Knowledge of the initial orientation of the two molecules in the pair could answer the first question. As suggested by F. Legay and N. Legay-Sommaire,¹⁴ for the diffusion of NO through a nitrogen matrix, a circular permutation of several molecules forming a ring (CINO, N_2 ..., N_2) could be suggested for the mechanism. The kinetic rate values obtained at 21, 22, and 23 K for the disappearance of the pair assuming an Arrhenius relationship $k = A \exp(-E_a/RT)$ allows us to determine the activation energy

for the first step of the process. It was found to be about (4 ± 0.5) kJ mole⁻¹.

Although the nitrogen crystal type is comparable to the argon crystal type, the nature of the matrix gas probably plays an important role in this phenomenon. Indeed in an argon matrix no pair is observed and weak dimer formation from the monomer occurs above 30 K. From the vibrational spectroscopy of NO and (NO)₂ isolated in solid neon, R. Kometer et al.¹⁵ identified also a van der Waals dimer (vdW) formed by two adjacent molecules and characterized by a single band, 17 cm⁻¹ red-shifted from the monomer absorption. However in this case the behavior of this species with temperature appeared very different from that of the X species. A reversible conversion of the cis dimer to the vdW dimer was observed between 5.9 and 9.4 K and attributed to the martensitic phase transition of solid neon for which a phase transition from fcc to hcp around 12 K has been reported. A phase transition inducing, in nitrogen, a change in orientation of ClNO monomer in the pair leading to isolated monomers or dimers does not seem likely. A nitrogen matrix is more rigid than solid neon, and no phase transition in the studied temperature range exists. Furthermore the observed process is not reversible, suggesting a diffusion process.

Long-Range Diffusion. A temperature increase above 26 K leads to an increase in the dimer/monomer ratio. Growth of the dimer occurs with a concomitant loss of intensity associated with the ClNO monomer. If we assume a random initial spatial distribution of reacting molecules for the diffusion-limited geminate recombination



the rate of the bimolecular reaction is second order and can be expressed by

$$\frac{-d[\text{ClNO}]}{dt} = k[\text{ClNO}]^2 \quad (2)$$

The integrated equation is

$$[\text{ClNO}]^{-1} - [\text{ClNO}_0]^{-1} = kt \quad (3)$$

where $[\text{ClNO}_0]$ is the initial monomer concentration (at $t = 0$) and $[\text{ClNO}]$ is the concentration of ClNO at time t if we assume that all ClNO monomers are mobile.

In this model where the two reacting molecules are random walkers, the reaction rate after a sufficiently long time can be represented by

$$k = 4 \Pi r_{\text{ClNO}} D \quad (4)$$

where D is the sum of diffusion coefficients of the two ClNO molecules in cm² s⁻¹ and r the ClNO–ClNO capture radius in centimeters.²⁴

In matrixes, the concentration of ClNO cannot be evaluated. The number of deposited molecules for a given sample thickness cannot be calculated because the value of the integrated absorption coefficient per molecule σ is unknown even in the gas phase. However, the relative integrated absorbance of ClNO (A) is proportional to the concentration and from the experimental values of the curves shown in Figure 8 we have plotted the reciprocal intensity of ClNO monomer versus time. As shown in Figure 9 the data collected at 26, 27, and 28 K fit eq 3 well. Values of k , in nonstandard units, are found to be $(1.37 \pm 0.1) \times 10^{-4}$, $(3.91 \pm 0.2) \times 10^{-4}$, and $(15 \pm 1) \times 10^{-4}$ cm min⁻¹ at 26, 27, and 28 K, respectively. Unfortunately, the

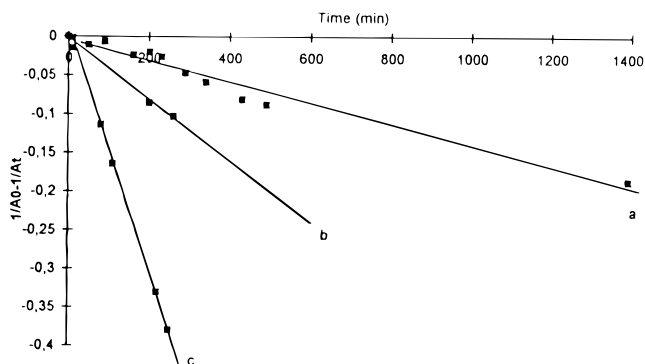


Figure 9. Plots of $1/A^0 - 1/A$ versus sample storage time at 26 K (a), 27 K (b), and 28 K (c) for a ClNO/N₂ (1/2000) sample. A^0 : ν_{NO} integrated intensity of monomer at initial time; A : ν_{NO} integrated intensity of monomer at time t .

diffusion coefficient cannot be evaluated for the reason invoked above: the absence of a value for σ . However, assuming an Arrhenius relationship these experimental values lead to an energy activation of about (7.5 ± 0.5) kJ mol⁻¹.

Effective rates could depend on the distance over which the ClNO molecule must move in order to find a reaction partner. In this view we have performed experiments at 27 and 28 K as described above but from a highly diluted sample (ClNO/N₂ = 1/10 000). A much smaller increase in the dimer/monomer ratio was observed compared to the more concentrated matrix but kinetic rates calculated from eq 3 were found to yield the same values as previously given, indicating that in this study the diffusion-controlled bimolecular rates do not depend on the spatial distribution of reactants over a time scale of 230 min.

As previously reported,¹⁶ the mobility of species in rare gas matrixes is enhanced in more amorphous matrixes formed at lower deposition temperature. No significant effect of the deposition temperature upon dimer formation was observed in this work probably due to restrictive experimental conditions in a nitrogen matrix, namely, the high recording temperature of 27 K which allows initially for the disappearance of matrix defects.

Acknowledgment. L.S.M. thanks Dr. J. R. Sodeau for reading the manuscript.

References and Notes

- (1) Brocklehurst, B.; Pimentel, G. C. *J. Chem. Phys.* **1962**, *36*, 2040.
- (2) Fournier, J.; Deson, J.; Vermeil, C.; Pimentel, G. C. *J. Chem. Phys.* **1979**, *70*, 5726.
- (3) Jacox, M. E. *Chem. Phys.* **1979**, *42*, 133; **1982**, *59*, 199.
- (4) Fournier, J.; Lalo, C.; Deson, J.; Vermeil, C. *J. Chem. Phys.* **1977**, *66*, 2656.
- (5) Lee, Y. P.; Pimentel, G. C. *J. Chem. Phys.* **1978**, *69*, 3063.
- (6) Feld, J.; Kuntu, H.; Apkarian, V. A. *J. Chem. Phys.* **1990**, *92*, 4826; **1993**, *93*, 1009.
- (7) Alimi, R.; Gerber, R. B.; Apkarian, V. A. *J. Chem. Phys.* **1990**, *92*, 3551.
- (8) Lawrence, W. G.; Apkarian, V. A. *J. Chem. Phys.* **1992**, *97*, 6199.
- (9) Ryan, E. T.; Weitz, E. *J. Chem. Phys.* **1993**, *99*, 1004.
- (10) Danilychev, A. V.; Apkarian, V. A. *J. Chem. Phys.* **1993**, *99*, 8617.
- (11) Krueger, K.; Weitz, E. *J. Chem. Phys.* **1992**, *96*, 2846.
- (12) Benderskii, A. V.; Wight, C. A. *J. Chem. Phys.* **1996**, *104*, 85.
- (13) Bahou, M.; Schriver-Mazzuoli, L.; Camy-Peyret, C.; Schriver, A.; Chiavassa, T.; Aycard, J. P. *Chem. Phys. Lett.* **1997**, *265*, 145.
- (14) Legay, F.; Legay-Sommaire, N. *Chem. Phys. Lett.* **1993**, *211*, 516.
- (15) Kometer, R.; Legay, F.; Legay-Sommaire, N.; Schwenter, N. *J. Chem. Phys.* **1994**, *100*, 8737.

- (16) Fairbrother, D. H.; La Brake, D.; Weitz, E. *J. Phys. Chem.* **1996**, *100*, 18848.
- (17) Ford, M. B.; Foxworthy, A. D.; Mains, G. J.; Raff, L. M. *J. Phys. Chem.* **1993**, *97*, 12134.
- (18) La Brake, D.; Weitz, E. *Chem. Phys. Lett.* **1993**, *211*, 430.
- (19) Stogard, A. *Chem. Phys. Lett.* **1975**, *36*, 357.
- (20) Jones, L. M.; Swanson, B. I. *J. Phys. Chem.* **1991**, *95*, 86.

- (21) Sanna, N.; Schrivier-Mazzuoli, L.; Hallou, A.; de Saxce, A.; Schrivier, A. *J. Chem. Phys.* **1995**, *103*, 6930.
- (22) Hallou, A.; Schrivier-Mazzuoli, L.; Schrivier, A.; Chaquin, P. *Chem. Phys.*, in press.
- (23) Hallou, A.; Schrivier-Mazzuoli, L.; Schrivier, A.; Sanna, N.; Pierretti, A. *Asian J. Spectrosc.* **1997**, *1*, 189.
- (24) Waite, T. R. *J. Chem. Phys.* **1960**, *32*, 21.